Smart Structures and Systems, *Vol. 32*, *No. 1* (*2023*) *37-47*
https://doi.org/10.12989/sss.2023.32.1.037

Teaching-learning-based strategy to retrofit neural computing toward pan evaporation analysis

Rana Muhammad Adnan Ikram [1a], Imran Khan[*2], Hossein Moayedi[**3,4], Loke Kok Foong [3,4b] and Binh Nguyen Le [3,4c]

[1] *School of Economics and Statistics*, *Guangzhou University*, *Guangzhou 510006*, *China*
[2] *Department of Economics*, *The University of Haripur*, *Pakistan*
[3] *Institute of Research and Development*, *Duy Tan University*, *Da Nang*, *Vietnam*
[4] *School of Engineering & Technology*, *Duy Tan University*, *Da Nang*, *Vietnam*

(*Received September 9*, *2020*, *Revised April 6*, *2023*, *Accepted July 7*, *2023*)

Abstract. Indirect determination of pan evaporation (PE) has been highly regarded, due to the advantages of intelligent models employed for this objective. This work pursues improving the reliability of a popular intelligent model, namely multi-layer perceptron (MLP) through surmounting its computational knots. Available climatic data of Fresno weather station (California, USA) is used for this study. In the first step, testing several most common trainers of the MLP revealed the superiority of the Levenberg-Marquardt (LM) algorithm. It, therefore, is considered as the classical training approach. Next, the optimum configurations of two metaheuristic algorithms, namely cuttlefish optimization algorithm (CFOA) and teaching-learning-based optimization (TLBO) are incorporated to optimally train the MLP. In these two models, the LM is replaced with metaheuristic strategies. Overall, the results demonstrated the high competency of the MLP (correlations above 0.997) in the presence of all three strategies. It was also observed that the TLBO enhances the learning and prediction accuracy of the classical MLP (by nearly 7.7% and 9.2%, respectively), while the CFOA performed weaker than LM. Moreover, a comparison between the efficiency of the used metaheuristic optimizers showed that the TLBO is a more time-effective technique for predicting the PE. Hence, it can serve as a promising approach for indirect PE analysis.

Keywords: environmental management; multi-layer perceptron; pan evaporation; teaching-learning-based optimization

1. Introduction

Pan evaporation (PE) is defined as an evaporative water loss from a standardized pan (Faiz *et al*. 2018). The PE plays a significant role in environmental management like water budgeting appraising (Malik *et al*. 2020) and approximating reference crop evapotranspiration (Malik *et al*. 2018). It is also an indication of the atmosphere evaporative demand (Djaman *et al*. 2017) and a reliable index for reference evapotranspiration analysis (Muhammad *et al*. 2019). So far, this parameter has been analyzed using various linear and non-linear techniques (Liu *et al*. 2004, Xu *et al*. 2006, Almedeij 2012). Shimi *et al*. (2020), for example, investigated various regressive tools for monthly and annual PE forecast. But the feasibility of machine learning approaches encouraged the authors to use the processors like artificial neural networks (ANN) (Kişi2009), adaptive neuro-fuzzy inference system (ANFIS) (Sanikhani *et al*. 2012), genetic programming (GP) (Guven and Kisi 2013), and support vector machine (SVM) (Lin *et al*. 2013) for indirectly analyze the PE, as well as other critical engineering domains (Hakim and Razak 2014, Ye *et al*. 2020).

Guven and Kişi (2011) applied linear GP (LGP), and compared its efficiency with several machine learning tools such as the MLP, GRNN, and RBF and found that the LGP can be successfully employed for modeling the PE. Goyal *et al*. (2014) investigated the feasibility of various intelligent and empirical models for the same purpose in Karso watershed, India. Their findings, first, revealed the higher potential of intelligent models, and second, the showed the superiority of least squares support vector regression (LS-SVR) and fuzzy logic. In this relation, The largest correlation for the fuzzy logic, LS-SVR, ANN1, and ANN2 was 0.82, 0.80, 0.72, and 0.75, respectively. Lu *et al*. (2018) employed various tree-based models including M5 model tree (M5Tree), gradient boosting decision tree (GBDT), and random forest (RF) for the same purpose in China. Their results showed that the GBDT, not only outperformed the empirical approaches but also was the superior model over the RF and M5Tree. Allawi and El-Shafie (2016) tested different ANFISs and RBFs for predicting the evaporation rate in southeast Malaysia. With reference to mean absolute error (MAE) of 0.0032 and the correlation of 0.963, the RBF presented the best performance. Mohammadrezapour

*Corresponding author, Ph.D.,
E-mail: imran@aup.edu.pk
**Co-corresponding author, Ph.D.,
E-mail: hosseinmoayedi@duytan.edu.vn
[a] Ph.D., E-mail: rana@gzhu.edu.cn
[b] Ph.D., E-mail: lokekokfoong@duytan.edu.vn
[c] Ph.D., E-mail: bnlnguyen@duytan.edu.vn

ISSN: 1738-1584 (Print), 1738-1991 (Online)

et al. (2019) compared the accuracy of SVM, ANFIS, and gene expression programming (GEP) for estimating the potential evapotranspiration in Sistan and Baluchestan stations, Iran. In all cases, the SVM was the best-fitted model, followed by the GEP and ANFIS. In a similar effort, the applicability of MLP, co-active ANFIS (CANFIS), RBF, and self-organizing map ANN were compared for the PE analysis in central Himalayas. The also considered Griffith's and Stephens-Stewart empirical models. Their findings revealed the better performance of the CANFIS and MLPNN (root mean square errors, RMSEs of 0.627 and 0.214, respectively). Another study for gratifying usage of the CANFIS was carried out by Salih *et al*. (2019).

Synthesizing different models has been extensively examined for creating innovative approaches. Keshtegar and Kisi (2017) presented a hybrid of response surface method (RSM) by synthesizing the exponential and polynomial mathematical functions to simulate the PE in Turkey stations. The compared the proposed model with several data mining tools including ANFIS, second-order response surface function, and M5Tree. It was shown that the RSM and M5Tree provide generally the best and poorest estimations, respectively. Qasem *et al*. (2019) could improve the accuracy of the SVR using wavelet transforms for predicting PE in Turkey. Keshtegar *et al*. (2016) used a conjugate gradient optimization to adjust nonlinear mathematical functions applied to the PE prediction problem in Iran. Based on the RMSEs of 1.94 vs. 2.41 and 2.19, the proposed model outperformed the ANFIS and M5Tree.

Concerning the use of metaheuristic algorithms, many scholars have used these strategies for optimizing predictive models in domains (Nehdi and Greenough 2007, Mehrabi *et al*. 2020, Asadi Nalivan *et al*. 2022). For environmental subjects, wind speed (Kerem and Saygin 2019), river bedload (Roushangar and Shahnazi 2019), dissolved oxygen concentration (Yaseen *et al*. 2018), flood susceptibility (Termeh *et al*. 2018), river flow (Yaseen *et al*. 2020) are examples of parameters that have been modeled by these techniques. Zeinolabedini Rezaabad *et al*. (2020) hybridized the ANFIS by several metaheuristic algorithms, namely imperialist competitive algorithm (ICA), biogeography-based optimization (BBO), teaching-learning–based optimization (TLBO), and invasive weed optimization (IWO) for evapotranspiration modeling. They showed that the ICA-ANFIS (RMSE = 0.5 and R = 0.99) is more accurate than other tested models. Likewise, Kisi *et al*. (2017) improved the quality of the ANFIS results using a dynamic evolving strategy. Moazenzadeh *et al*. (2018) used a combination of SVR with firefly algorithm (FA) for simulating the evaporation in Iran. It was observed that the prediction error of the FA-SVR was in a shorter range ([1.02, 1.31] vs. [1.05, 1.43]). In a similar optimization task, Guan *et al*. (2020) hybridized the SVR using krill herd algorithm. They successfully predicted the PE. A comparative study by Tikhamarine *et al*. (2019) evaluated the competency of five metaheuristic algorithms, namely grey wolf optimizer (GWO), multi-verse optimizer (MVO), particle swarm optimizer (PSO), whale optimization algorithm (WOA) and ant lion optimizer (ALO), coupled with the ANN for reference evapotranspiration prediction in India and Algeria. They professed the higher robustness of the GWO, due to its higher accuracy in both stations. More application of these algorithms can be found in studies like (Ali Ghorbani *et al*. 2018, Feng *et al*. 2018).

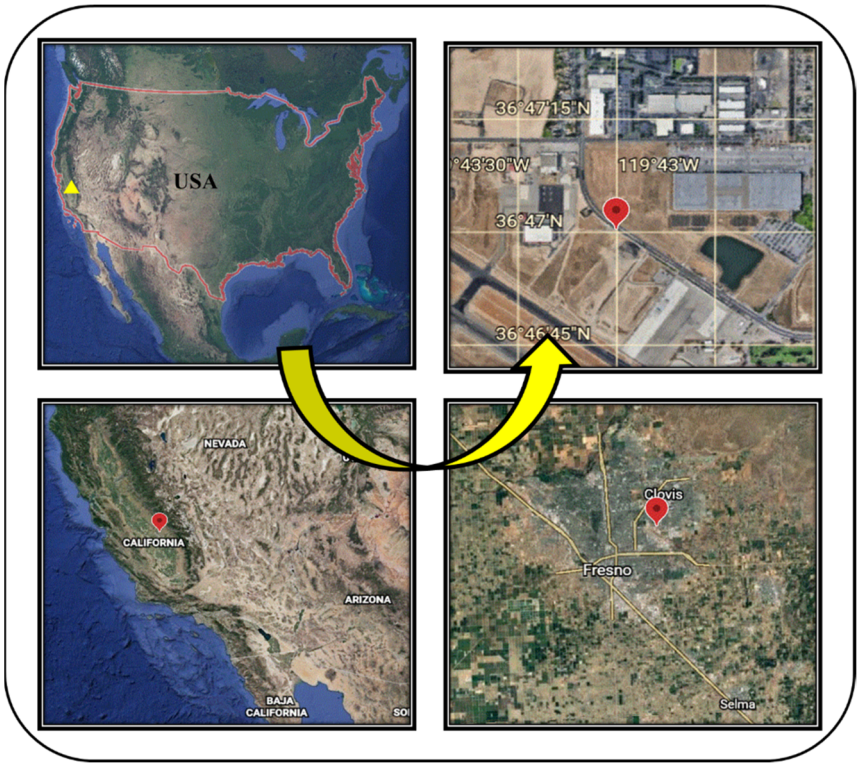

Fig. 1 Location of the Fresno station

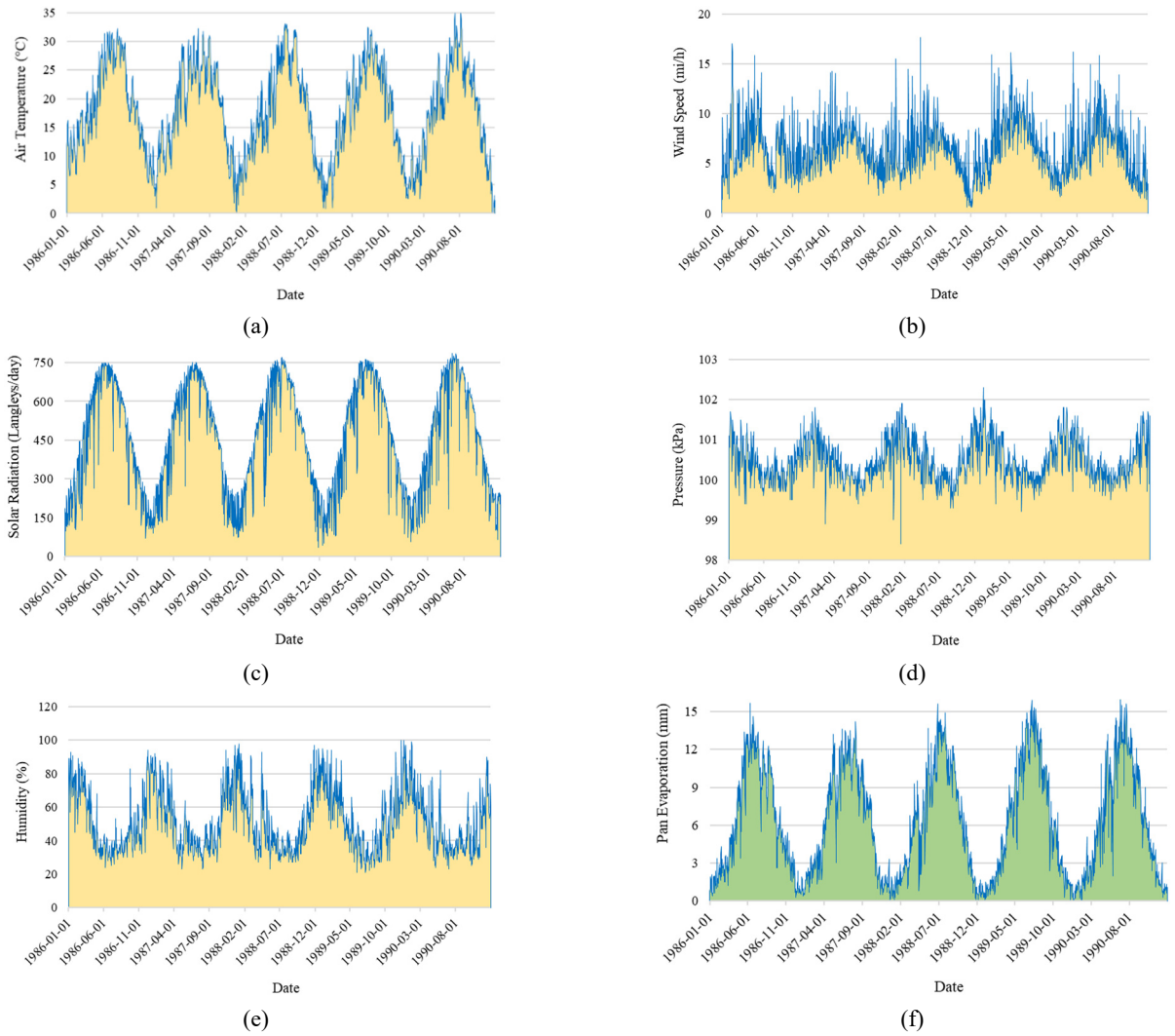

Fig. 2 Time-series of the PE and effective factors

In more recent works by Moayedi *et al*. (2021) and Zhang *et al*. (2022), several algorithms including shuffled complex evolution (SCE), vortex search algorithms (VSA), sunflower optimization (SFO), electromagnetic field optimization (EFO), and stochastic fractal search (SFS) were comparatively and successfully tested on ANN for predicting PE. Following these innovative efforts, this work evaluates the feasibility of two novel strategies, namely cuttlefish optimization algorithm (CFOA) and teaching-learning-based optimization (TLBO) for training the ANN applied to predicting the PE from various climatic parameters. With reference to the earlier literature, the reason for utilizing such algorithms lies in their potential for overcoming computational knots like local minima trap (Moayedi *et al*. 2019, 2020). The results are compared with a typically trained neural network to assess the effects of the proposed approaches.

2. Methodology and study area

In this work, the PE is predicted by taking the effect of several climatic parameters into account. These parameters are air temperature (T_A), wind speed (S_W), solar radiation (R_S), pressure (P), and the percentage of humidity (H_P) which play the role of inputs during the development of intelligent models. In this relation, the PE is the target parameter.

The data are collected in a weather station, namely Fresno with the WBAN number of 93193. Fig. 1 shows the location of this station in California (Longitude: 119° 43' W and Latitude: 36° 47' N). The Santa Maria station is operated by the US environmental protection agency and its records are downloaded from the corresponding website (http://www.epa.gov).

Considering the available for the last five-year, the records from January 01, 1986 to December 31, 1989 are used by models to learn the non-linear pattern of the PE. Once the models are trained, they predict the PE for the inputs of the subsequent year, i.e., January 01, 1990 to December 31, 1990. Comparing the predicted PEs with the actual values recorded for this period will reflect the reliability of the developed models in confronting new climatic conditions.

Fig. 2 presents the variations of the T_A, S_W, R_S, P, H_P, and PE over 1986-1990. As expected, T_A, R_S, and PE follow

Table 1 Descriptive statistics of the PE and input factors in both periods

Phase	Parameter	Indicator					
		Average	Skewness	Sample variance	Standard deviation	Minimum	Maximum
Training	T_A (°C)	17.9	-0.1	62.9	7.9	0.2	33.1
	S_W (mi/h)	6.5	0.6	6.8	2.6	0.6	17.6
	R_S (Langley)	453.7	-0.2	42459.3	206.1	35.1	769.5
	P (Kpa)	100.5	0.4	0.3	0.5	98.4	102.3
	H_P (%)	51.9	0.6	335.1	18.3	21.0	100.0
	PE (mm)	6.2	0.3	18.4	4.3	0.0	15.9
Testing	T_A (°C)	17.5	-0.1	72.7	8.5	-3.0	34.9
	S_W (mi/h)	6.6	0.5	8.2	2.9	1.3	16.2
	R_S (Langley)	468.1	-0.1	41152.2	202.9	66.0	788.6
	P (Kpa)	100.5	0.7	0.2	0.5	99.5	101.8
	H_P (%)	49.0	0.7	269.6	16.4	23.0	99.0
	PE (mm)	6.4	0.3	19.6	4.4	0.0	16.1

a distinct pattern in this period. The average value of the PE for 1986, 1987, 1988, 1989, and 1990 is 6.2, 6.1, 6.1, 6.3, and 6.4 *mm*. Moreover, the maximum evaporation occurred is 16.1 *mm* on June 27. The statistical description of all parameters for the training and testing periods is presented in Table 1.

2.1 Methodology

The MLPNN: The MLPNN (Hornik *et al*. 1989, Pinkus 1999) is a highly popular neural network that can deeply explore non-linear relationships. Similar to a biological neural system, several neurons, that are thoroughly connected by weights, form an ANN (Anderson and McNeill 1992). Based on the layer that they lie in, each group of neurons is labeled as one of input, hidden, output. The weights are tantamount to the synapses that (for a three-layered MLPNN) make connections between the input neurons with the hidden neurons, as well as between the hidden neurons with output neurons. Along with a number of bias factors, the weights affect the input vector in each neuron. Another important component of a neuron is the activation function which activates the final calculations prior to being released. Note that, this function could be either linear (e.g., Purelin) or non-linear (e.g., Tansig) for each layer (Nguyen *et al*. 2019, Mehrabi 2021).

Fig. 3 shows the MLPNN used for predicting the PE in the present work. Based on the five input parameters (i.e., T, WS, SR, P, and H) and one output parameter, this network has five neurons in the first layer, and one neuron in the latest layer. The number of hidden neurons was designated to be four after a trial and error process.

Generally, an MLPNN is trained through adjusting the biases and weights to establish a reasonable input-output mathematical relationship (Mehrabi and Moayedi 2021). In the Matlab environment, various training algorithms can handle this task.

The CFOA: Based on the camouflage behavior of the cuttlefish, Eesa *et al*. (2013) developed the CFOA

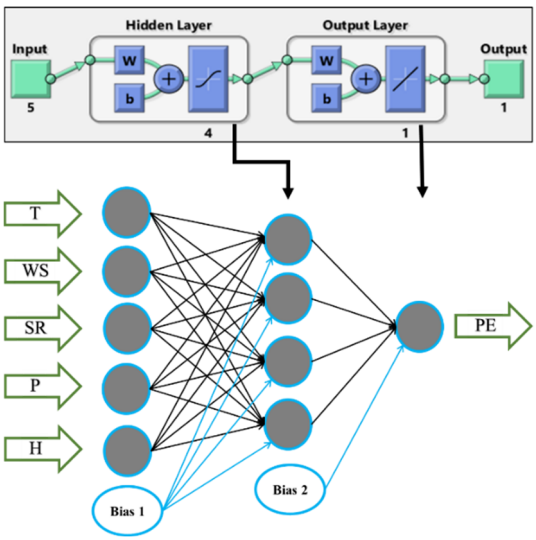

Fig. 3 The MLPNN used for simulating the PE

algorithm. This technique has provided a capable optimizer for diverse complex issues (Giernacki *et al*. 2017, Eesa and Orman 2020). The actions in three cell layers of a cuttlefish, namely chromatophores, iridophores, and leucophores are considered for this process. Reflection and visibility are two major procedures that do the homochromy. The first procedure shows how the cuttlefish reflects an incoming light and the second one how the cuttlefish matches the color of its skin with the environment. Hence, the algorithm seeks the best hiding state.

As equation 1 expresses, in the first step of the CFOA, a population (P) is initialized with d chromatophore cells each of which containing N points.

$$P = (S_i)_{1\le i\le d} = (Cell^i)_{1\le i\le d} = (point_{i,j})_{(1\le i\le d, 1\le j\le N)} \quad (1)$$

Next, new solutions are created from the existing ones. The population is classified in four classes where the global

and local search tasks are cooperatively handled by the classes 2 and 3, and 1 and 4, respectively. the individuals of class 1 simulate the chromatophore-iridophore interaction to reflect the light with respect to the surrounding light colors. Equations 2 and 3 are used to address the new solution points.

$$Reflection_j = R \times point_{i,j} \quad (2)$$

$$Visibility_j = V \times (pointp_j - point_{i,j}) \quad (3)$$

Also, S_{new} is defined as follows

$$S_{new} = Visibility + Reflection \quad (4)$$

The terms R and V, which represent the degree of reflection and visibility, respectively, are calculated as follows

$$R = rand \times (r_1 - r_2) + r_2 \quad (5)$$

$$V = rand \times (v_1 - v_2) + v_2 \quad (6)$$

where *rand* is a random number in [0, 1], r_1 and r_2, as well as v_1 and v_2, are the limits for the mentioned parameters. Notably, R should be computed for this class, while V equals 1.

In the second class, the individuals mark the iridophore cells to simulate the reflection of the outside light. The reflection can be taken by the chromatophore cells or released to outside. In this class, Eq. (3) is used to calculate the visibility, while the reflection is obtained from Eq. (7).

$$reflection_j = R \times bestp_j \quad (7)$$

In the third class, without any change in the color, the leucophore characteristic reflecting light taken from the chromatophore cells is used. The reflection of the newly-generated solutions is calculated by Equation 7. The visibility is obtained as follows

$$visibility_j = V \times (bestp_j - AV_{best}) \quad (8)$$

where AV_{best} is average of the S_{best}. In the case of this class, V is calculated whereas R equals 1.

Lastly, in the fourth class, the reflection case of the outside light is simulated. The CFOA checks the suitability of the found solution. If the fitness of the S_{best} is higher than the present solution, the are exchanged, otherwise, the explained procedure continues until meeting a stopping criterion (Riffi and Bouzidi 2015).

The TLBO: Mimicking the common teaching-learning process in schools, the TLBO was designed by Rao *et al*. (2011) in 2011. This algorithm has successfully served in various engineering domains (Zhang *et al*. 2020, Zhou *et al*. 2020). Consisting of two phases of teacher and learner, a teacher tries to establish the largest possible harmony over the learning community (i.e., the students).

In the teacher phase, the most outstanding learner is deemed as the teacher. The i^{th} student in the t^{th} iteration is updated based on the below equation

$$X_i^{t+1} = X_i^t + r_i(X_{teacher}^t - T_i^f X_{ave}) \quad (9)$$

where X_i^t represents the current solution, r_i gives a random value in [0, 1], $X_{teacher}^t$ stands for the most outstanding solution (i.e., the teacher), and X_{ave} is the average result of the students. Also, T_i^f is the teaching factor that obtained as follows

$$T_i^f = round[1 + rand(0,1)\{2 - 1\}] \quad (10)$$

The second phase is dedicated to the interaction between the students. They aim to enhance their knowledge through this scientific interaction. Mathematically, assuming the students X_j and X_k ($k \neq j$), it can be written

$$\begin{aligned} &X_i^{t+1} = X_i^t + r_i\left(X_j^{t+1} - X_k^{t+1}\right) \\ &\text{if} \quad f(X_k^{t+1}) > f\left(X_j^{t+1}\right) \end{aligned} \quad (11)$$

$$\begin{aligned} &X_i^{t+1} = X_i^t + r_i\left(X_k^{t+1} - X_j^{t+1}\right) \\ &\text{if} \quad f\left(X_j^{t+1}\right) > f(X_k^{t+1}) \end{aligned} \quad (12)$$

Once the new solution is of higher quality (compared to the present solution), it replaces the present solution (Sayari *et al*. 2020).

3. Results and discussion

3.1 Accuracy indicators

Different statistical accuracy indices are used to assess the quality of prediction and comparing the performance of the models. The goodness of fit of the results is reflected by Pearson correlation coefficient (PCC) as expressed in Eq. (13). Needless to say, the larger the obtained PCC is, the higher the agreement of the results is

$$PCC = \frac{\sum_{i=1}^{S}(PE_{i_{forecast}} - \overline{PE}_{forecast})(PE_{i_{reality}} - \overline{PE}_{reality})}{\sqrt{\sum_{i=1}^{S}(PE_{i_{forecast}} - \overline{PE}_{forecast})^2}\sqrt{\sum_{i=1}^{S}(PE_{i_{reality}} - \overline{PE}_{reality})^2}} \quad (13)$$

Moreover, the error of prediction is measured by two criteria, namely mean absolute error (MAE) and root mean square error (RMSE) as expressed in Eqs. (14) and (15).

$$MAE = \frac{1}{S}\sum_{i=1}^{S}|PE_{i_{reality}} - PE_{i_{forecast}}| \quad (14)$$

$$RMSE = \sqrt{\frac{1}{S}\sum_{i=1}^{S}[(PE_{i_{reality}} - PE_{i_{forecast}})]^2} \quad (15)$$

In the above formulations, applied to *S* samples,

Table 2 The results of trying various training algorithms

Algorithm	Description	RMSE	
		Train	Test
Trainbfg	BFGS Quasi-Newton	0.2098	0.2319
Traincgb	Conjugate Gradient with Powell/Beale Restarts	0.2382	0.2800
Traincgf	Fletcher-Powell Conjugate Gradient	0.2159	0.2291
Traincgp	Polak-Ribiére Conjugate Gradient	0.2854	0.3418
Traingdx	Variable Learning Rate Backpropagation	0.3845	0.4225
Trainoss	One Step Secant	0.2918	0.3343
Trainscg	Scaled Conjugate Gradient	0.3631	0.3424
Trainrp	Resilient Backpropagation	0.3560	0.4478
Trainlm	Levenberg-Marquardt	0.1989	0.2134

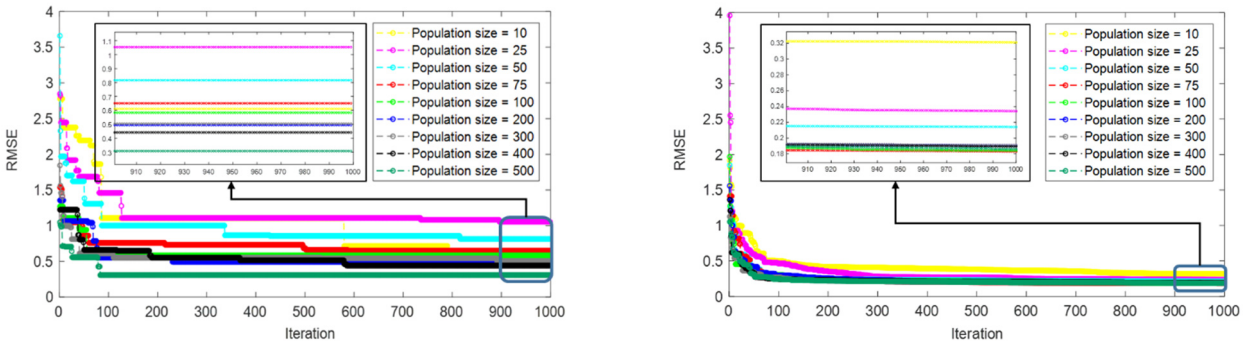

(a) (b)

Fig. 4 The convergence proceeding of (a) MLP-CFOA; and (b) MLP-TLBO

$PE_{i_{reality}}$ and $PE_{i_{forecast}}$ stand for the observed and predicted PE, respectively. Based on the considered periods, S equals 1461 and 365 in the training and testing phase, respectively.

3.2 Classical training

First, to determine the best typical training algorithm for the ANN, this network was trained by nine different existing algorithms, namely trainbfg, traincgb, traincgf, traincgp, traingdx, trainoss, trainscg, trainrp, and trainlm. Notably, Matlab v. 2017b is used for the implementations in this study. Table 2 gives the results of this process.

According to this table, with the RMSEs of 0.1989 and 0.2134 for the training and testing phase, respectively, trainlm (i.e., Levenberg- Marquardt (Moré 1978)) performs the best among the tested algorithms. The neural network adjusted by this algorithm is used and referred to as the typical MLP (TMLP) for further evaluations.

3.3 Metaheuristic-based training

Applying the CFOA and TLBO to the MLP is the purpose of this section. Two hybrids of MLP-CFOA and MLP-TLBO are implemented to investigate the capability of metaheuristic techniques versus typical training algorithms. In this process, the CFOA and TLBO pursue the optimal minimization of the problem function which is defined as the RMSE between the observed PEs and those predicted by the MLP neural network. Note that, the data belonging to the training period are used in this stage.

As a well-established step in utilizing population-based algorithms, a trial and error practice is executed for designating a suitable population size (N_P, e.g., the number of students in the TLBO). Nine values including 10, 25, 50, 75, 100, 200, 300, 400, and 500 are tested as the N_Ps of the MLP-CFOA and MLP-TLBO. Fig. 4 shows the resultant convergence curves. As is seen, this parameter has a distinct effect on the optimization process. For example, the performance of the N_P = 25 is considerably weaker than others. The N_Ps of 500 and 75 are finally chosen for the MLP-CFOA and MLP-TLBO, due to the lowest RMSEs obtained for them.

3.4 Training efficiency and formulation

The RMSEs of the MLP-CFOA and MLP-TLBO were 0.3081 and 0.1832, respectively. This accuracy indicator along with the MAEs of 0.2239 and 0.1399 indicates a very good level of accuracy for both models. It means that the ANN trained by both metaheuristic algorithms has acquired a correct perception from the PE behavior. As for the TMLP, the LM could train it with the RMSE and MAE of 0.1989 and 0.1516, respectively. It similarly shows the high capability of this algorithm for analyzing the behavior of the PE from T_A, S_W, R_S, P, and H_P.

Fig. 5 shows the training results. The pattern comparison shows that the changes in the PE have been correctly predicted over all four years. Moreover, the presented histogram charts show a desirable frequency of errors. At a glance, the frequency of the errors reduces with the increase of the magnitudes.

A simple comparison between these three MLPs demonstrates that one of the metaheuristic-trained networks captures a more profound understanding than the TMLP. More clearly, the TLBO-adjusted weights and biases are the most reliable ones for setting the MLP up. After that, the LM outperformed the CFOA.

Eq. (16) gives the relationship suggested by the TLBO for predicting the PE.

$$\begin{aligned} PE_{TLBO} = {} & 0.515480 \times g\left(R_{Hid_1}\right)| \\ & +0.486265 \times g\left(R_{Hid_2}\right) \\ & -0.215546 \times g\left(R_{Hid_3}\right) \\ & +0.310956 \times g\left(R_{Hid_4}\right) \\ & -0.657627 \times g\left(R_{Hid_5}\right) + 0.412092 \end{aligned} \tag{16}$$

where $g(x) = \frac{2}{1+e^{-2x}} - 1$ is the activation function. Also, $R_{Hid_1}, R_{Hid_2}, R_{Hid_3}$, and R_{Hid_4} contribute to the inputs through the following equations:

$$\begin{aligned} R_{Hid_1} = {} & 0.834459 \times T_A - 1.067082 \times S_W \\ & -0.907805 \times R_S - 0.949503 \times P \\ & +0.412931 \times H_P - 1.931622 \end{aligned} \tag{17}$$

$$\begin{aligned} R_{Hid_2} = {} & 0.967031 \times T_A - 0.527909 \times S_W \\ & -1.121571 \times R_S - 0.186468 \times P \\ & -1.106545 \times H_P - 0.965811 \end{aligned} \tag{18}$$

$$\begin{aligned} R_{Hid_3} = {} & -0.897107 \times T_A - 0.112751 \times S_W \\ & +1.099499 \times R_S + 0.999855 \times P \\ & +0.839666 \times H_P + 0.000000 \end{aligned} \tag{19}$$

$$\begin{aligned} R_{Hid_4} = {} & 0.987260 \times T_A + 1.092657 \times S_W \\ & -0.034927 \times R_S + 0.697875 \times P \\ & +1.036500 \times H_P - 0.965811 \end{aligned} \tag{20}$$

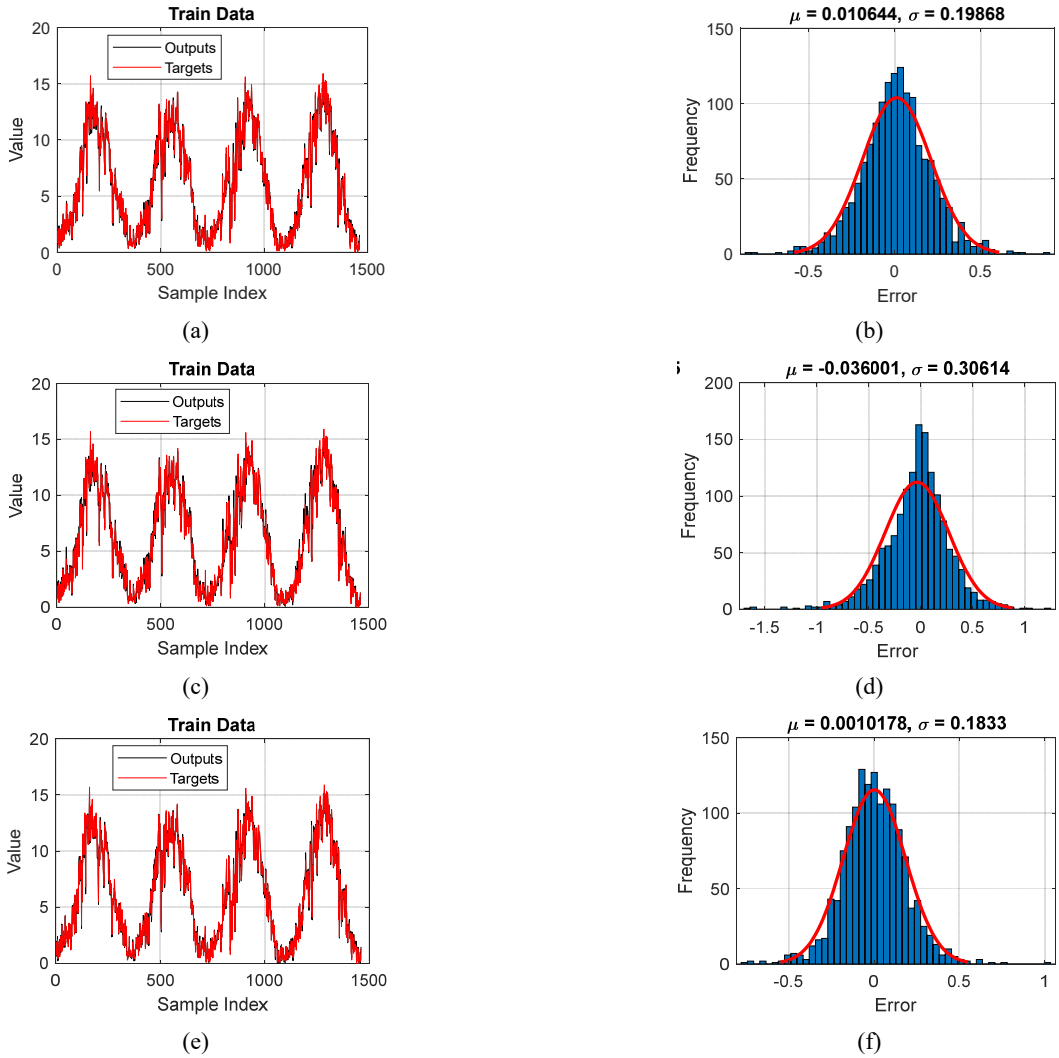

Fig. 5 Real and captured PE patterns and histogram of the errors for the training samples of (a) and (b) TMLP; (c) and (d) MLP-CFOA; and (e) and (f) MLP-TLBO (μ = Mean error and σ = Standard error)

$$R_{Hid_5} = 0.339569 \times T_A + 1.192675 \times S_W + 0.770372 \times R_S + 1.178831 \times P + 0.458546 \times H_P + 1.931622 \quad (21)$$

3.5 Predicting the PE

In this section, the accuracy of the proposed models (i.e., the TMLP, MLP-CFOA, and MLP-TLBO) is evaluated for predicting the PE over the year 1990. With this in mind that the models have not previously come across these data, the accuracy of their prediction addresses their ability for reproducing the PE pattern.

Fig. 6 gives a comparison between the observed and predicted PEs in the testing phase. Similar to the training phase, the models have been highly sensitive to the changes in both large and small scales. The highest PE value is 16.1 that is predicted to be 15.5926, 15.1157, and 15.5462 by the TMLP, MLP-CFOA, and MLP-TLBO, respectively. As for the lowest value, the PE of 0.0 is predicted to be 0.2070, 0.1254, and 0.0757.

Referring to the RMSEs of 0.2134, 0.3194, and 0.2029, plus the MAEs of 0.1623, 0.2332, and 0.1473, a reliable prediction has been carried out by all three models. Moreover, the values of mean absolute percentage error were below 7% (i.e., 5.2580, 6.6022, and 5.5532%) which reflect a low relative error. Therefore, it can be deduced that LM, CFOA, and TLBO have properly tuned the computational parameters so that they can be reliably used for unseen climatic situations.

The third accuracy indicator is the PCC that measured the goodness of fit for both training and testing results. The regression charts are shown in Fig. 7. Each figure contains the training and testing results of one model. As is seen, in all cases, the models are very close to the ideal prediction (i.e., the line with the equation $x = y$). The PCCs were 0.99896, 0.99745, and 0.99909 for the training results, and 0.99892, 0.99740, and 0.99895 for the testing results.

3.6 Comparison and further discussion

In the former section, it was derived that the TLBO gives the best training of the MLP, followed by the LM and CFOA. The same ranks were obtained for the testing phase, due to the higher reliability of the MLP-TLBO compared to both TMLP and MLP-CFOA. Accordingly, the use of TLBO increased the learning capability of the MLP by around 7.7% in terms of the MAE. Likewise, the TLBO-based network could predict the PE with nearly 9.2% lower error. Moreover, although the CFOA could develop a very robust MLP, the results of the typical MLP were more

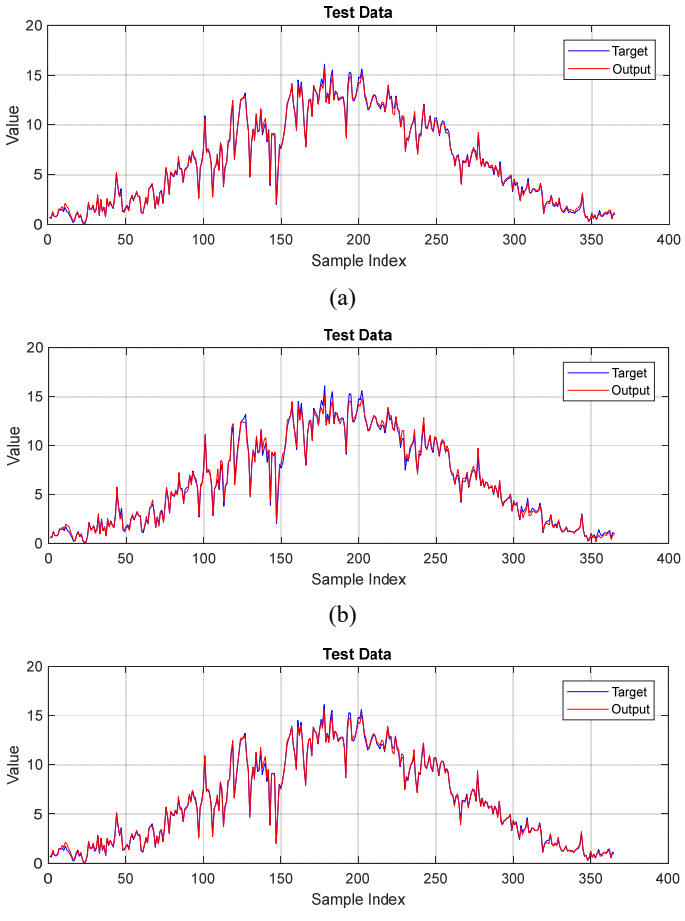

Fig. 6 Comparison between the observed PEs and those predicted by (a) TMLP; (b) MLP-CFOA; and (c) MLP-TLBO in the testing phase

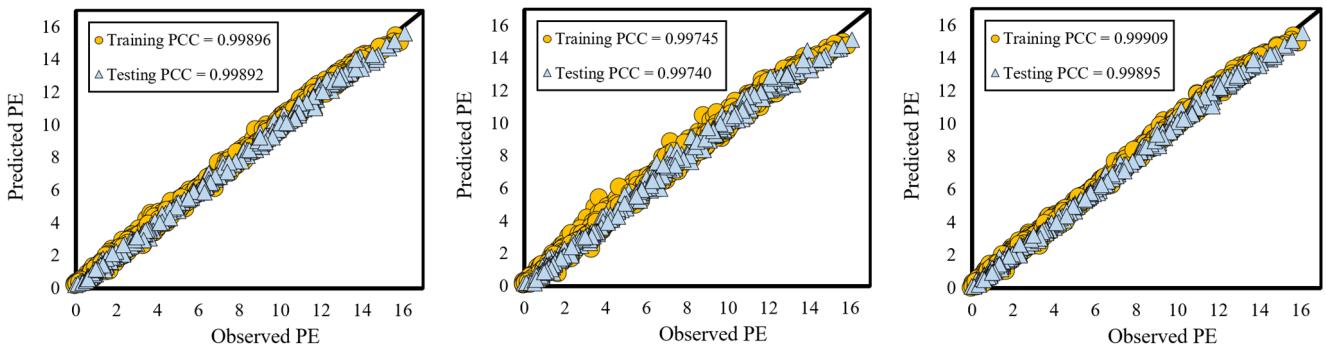

Fig. 7 Agreement between the observed PEs and those predicted by (a) TMLP; (b) MLP-CFOA; and (c) MLP-TLBO in both phases

promising.

Another advantage of the TLBO was utilizing a considerably simpler configuration compared to the CFOA (i.e., the N_Ps of 75 vs. 500). Consequently, the optimization of the MLP using the TLBO was faster than the other optimizer (1491.4 vs. 4602.3 seconds). Referring to Fig. 4, it is true that the accuracy of the CFOA algorithm has increased with the increase of population size but it should be considered that the sensitivity becomes less and less. In other words, the rate of accuracy increment is much larger for the initial population. Therefore, based on this observation, as well as previous studies of the CFOA algorithm, we deduced that population sizes greater than 500 would not add too much to the solution. Besides, since optimization using these algorithms is a time-consuming process, time should be considered as well. As is known, higher population sizes require longer time. Hence, even if heavier population sizes give a better response, it would not be quite optimum from computational point of view.

The limitations of this research can be considered as potential ideas for conducting future studies. For instance, although the high generalizability was observed for the suggested models, they were applied only to one station. For further reliability assessment, cross-validations are recommended using the similar records of other stations. It exposes different meteorological and environmental conditions for adapting the models. Moreover, the problem space in this work was constructed from 5 inputs. It raises the idea of feature selection for reducing the most eminent inputs and discarding the negligible ones. Sometimes it can result in a less complicated configuration, and consequently, reducing the computational burden of the problem (e.g., reducing the optimization time).

4. Conclusions

Despite the excellent applicability of popular PE evaluative models, they can be further enhanced by assigning their training task to metaheuristic science. This research evaluated the potential of cuttlefish optimization algorithm and teaching-learning-based optimization for training an MLP neural network. Comparing these algorithms with a well-known trainer revealed that the relationship between the PE and T, WS, SR, P, and H is better understood by the TLBO-based model. It also outperformed two other models in predicting this parameter in terms of all accuracy indicators. Therefore, replacing the LM with the TLBO is an effective way for enhancing the accuracy of the MLP. However, the LM was superior over the CFOA in both phases. Furthermore, compared to the CFOA, the solution of the TLBO was discovered in a shorter time and by a smaller number of agents. Therefore, this algorithm could optimize the MLP in a less complicated space. Last but not least, the authors would suggest comprehensive comparative studies toward identifying more powerful optimizers.

Acknowledgments

This work was supported by the General Projects of Guangdong Natural Science Research Projects (grant number 2023A1515011520).

References

Ali Ghorbani, M., Kazempour, R., Chau, K.W., Shamshirband, S. and Taherei Ghazvinei, P. (2018), "Forecasting pan evaporation with an integrated artificial neural network quantum-behaved particle swarm optimization model: a case study in Talesh, Northern Iran", *Eng. Applicat. Computat. Fluid Mech.*, **12**(1), 724-737. https://doi.org/10.1080/19942060.2018.1517052

Allawi, M.F. and El-Shafie, A. (2016), "Utilizing RBF-NN and ANFIS methods for multi-lead ahead prediction model of evaporation from reservoir", *Water Resour. Manage.*, **30**(13), 4773-4788. https://doi.org/10.1007/s1126900-016-1452-1

Almedeij, J. (2012), "Modeling pan evaporation for Kuwait by multiple linear regression", *Scientif. World J.*, **2012**. https://doi.org/10.1100/2012/574742

Anderson, D. and McNeill, G. (1992), "Artificial neural networks technology", *Kaman Sci. Corp.* **258**(6), 1-83.

Asadi Nalivan, O., Mousavi Tayebi, S.A., Mehrabi, M., Ghasemieh, H. and Scaioni, M. (2022), "A hybrid intelligent model for spatial analysis of groundwater potential around Urmia Lake, Iran", *Stoch. Environ. Res. Risk Assess.*. **37**, 1821-1838. https://doi.org/10.1007/s00477-022-02368-y

Djaman, K., Koudahe, K. and Ganyo, K.K. (2017), "Trend analysis in annual and monthly pan evaporation and pan

coefficient in the context of climate change in togo", *J. Geosci. Environ. Protection*, **5**(12), 41-56. https://doi.org/10.4236/gep.2017.512003

Eesa, A.S., Brifcani, A.M.A. and Orman, Z. (2013), "Cuttlefish algorithm-a novel bio-inspired optimization algorithm", *Int. J. Scientif. Eng. Research* **4** (9), 1978-1986.

Eesa, A.S. and Orman, Z. (2020), "A new clustering method based on the bio-inspired cuttlefish optimization algorithm", *Expert Syst.*, **37**(2), e12478. https://doi.org/10.1111/exsy.12478

Faiz, M.A., Liu, D., Fu, Q., Wrzesiński, D., Baig, F., Nabi, G., Khan, M.I., Li, T. and Cui, S. (2018), "Extreme precipitation and drought monitoring in northeastern China using general circulation models and pan evaporation-based drought indices", *Climate Res.*, **74**(3), 231-250. https://doi.org/10.3354/cr01503

Feng, Y., Jia, Y., Zhang, Q., Gong, D. and Cui, N. (2018), "National-scale assessment of pan evaporation models across different climatic zones of China", *J. Hydrol.*, **564**, 314-328. https://doi.org/10.1016/j.jhydrol.2018.07.013

Giernacki, W., Espinoza Fraire, T. and Kozierski, P. (2017), "Cuttlefish optimization algorithm in autotuning of altitude controller of unmanned aerial vehicle (UAV)", In: *Iberian Robotics Conference*, pp. 841-852. https://doi.org/10.1007/978-3-319-70833-1_68

Goyal, M.K., Bharti, B., Quilty, J., Adamowski, J. and Pandey, A. (2014), "Modeling of daily pan evaporation in sub tropical climates using ANN, LS-SVR, Fuzzy Logic, and ANFIS", *Expert Syst. Applicat.*, **41**(11), 5267-5276. https://doi.org/10.1016/j.eswa.2014.02.047

Guan, Y., Mohammadi, B., Pham, Q.B., Adarsh, S., Balkhair, K.S., Rahman, K.U., Linh, N.T.T. and Tri, D.Q. (2020), "A novel approach for predicting daily pan evaporation in the coastal regions of Iran using support vector regression coupled with krill herd algorithm model", *Theor. Appl. Climatol.*, 1-19. https://doi.org/10.1007/s00704-020-03283-4

Guven, A. and Kişi, Ö. (2011), "Daily pan evaporation modeling using linear genetic programming technique", *Irrig. Sci.*, **29**(2), 135-145. https://doi.org/10.1007/s00271-010-0225-5

Guven, A. and Kisi, O. (2013), "Monthly pan evaporation modeling using linear genetic programming", *J. Hydrol.*, **503**, 178-185. https://doi.org/10.1016/j.jhydrol.2013.08.043

Hakim, S.J.S. and Razak, H.A. (2014), "Modal parameters based structural damage detection using artificial neural networks-a review", *Smart Struct. Syst., Int. J.*, **14**(2), 159-189. https://doi.org/10.12989/sss.2014.14.2.159

Hornik, K., Stinchcombe, M. and White, H. (1989), "Multilayer feedforward networks are universal approximators", *Neural Networks*, **2**(5), 359-366. https://doi.org/10.1016/0893-6080(89)90020-8

Kerem, A. and Saygin, A. (2019), "Scenario-based wind speed estimation using a new hybrid metaheuristic model: Particle swarm optimization and radial movement optimization", *Measur. Control*, **52**(5-6), 493-508. https://doi.org/10.1177/0020294019842597

Keshtegar, B. and Kisi, O. (2017), "Modified response-surface method: new approach for modeling pan evaporation", *J. Hydrol. Eng.*, **22**(10), 04017045. https://doi.org/10.1061/(ASCE)HE.1943-5584.0001541

Keshtegar, B., Piri, J. and Kisi, O. (2016), "A nonlinear mathematical modeling of daily pan evaporation based on conjugate gradient method", *Comput. Electron. Agricul.*, **127**, 120-130. https://doi.org/10.1016/j.compag.2016.05.018

Kişi, Ö. (2009), "Daily pan evaporation modelling using multi-layer perceptrons and radial basis neural networks", *Hydrol. Processes: Int. J.*, **23**(2), 213-223. https://doi.org/10.1002/hyp.7126

Kisi, O., Mansouri, I. and Hu, J.W. (2017), "A new method for evaporation modeling: dynamic evolving neural-fuzzy inference system", *Adv. Meteorol.*, **2017**. https://doi.org/10.1155/2017/5356324

Lin, G.F., Lin, H.Y. and Wu, M.C. (2013), "Development of a support-vector-machine-based model for daily pan evaporation estimation", *Hydrol. Processes*, **27**(22), 3115-3127. https://doi.org/10.1002/hyp.9428

Liu, B., Xu, M., Henderson, M. and Gong, W. (2004), "A spatial analysis of pan evaporation trends in China, 1955–2000", *J. Geophys. Res.: Atmospheres*, **109**(D15). https://doi.org/10.1029/2004JD004511

Lu, X., Ju, Y., Wu, L., Fan, J., Zhang, F. and Li, Z. (2018), "Daily pan evaporation modeling from local and cross-station data using three tree-based machine learning models", *J. Hydrol.*, **566**, 668-684. https://doi.org/10.1016/j.jhydrol.2018.09.055

Malik, A., Kumar, A. and Kisi, O. (2018), "Daily pan evaporation estimation using heuristic methods with gamma test", *J. Irrig. Drain. Eng.*, **144**(9), 04018023. https://doi.org/10.1061/(ASCE)IR.1943-4774.0001336

Malik, A., Rai, P., Heddam, S., Kisi, O., Sharafati, A., Salih, S.Q., Al-Ansari, N. and Yaseen, Z.M. (2020), "Pan evaporation estimation in Uttarakhand and Uttar Pradesh States, India: validity of an integrative data intelligence model", *Atmosph.*, **11**(6), 553. https://doi.org/10.3390/atmos11060553

Mehrabi, M. (2021), "Landslide susceptibility zonation using statistical and machine learning approaches in Northern Lecco, Italy", *Natural Hazards*, 1-37. https://doi.org/10.1007/s11069-021-05083-z

Mehrabi, M. and Moayedi, H. (2021), "Landslide susceptibility mapping using artificial neural network tuned by metaheuristic algorithms", *Environ. Earth Sci.*, **80**(24), 1-20. https://doi.org/10.1007/s12665-021-10098-7

Mehrabi, M., Pradhan, B., Moayedi, H. and Alamri, A. (2020), "Optimizing an adaptive neuro-fuzzy inference system for spatial prediction of landslide susceptibility using four state-of-the-art metaheuristic techniques", *Sensors*, **20**(6), 1723. https://doi.org/10.3390/s20061723

Moayedi, H., Mehrabi, M., Mosallanezhad, M., Rashid, A.S.A. and Pradhan, B. (2019), "Modification of landslide susceptibility mapping using optimized PSO-ANN technique", *Eng. Comput.*, **35**(3), 967-984. https://doi.org/10.1007/s00366-018-0644-0

Moayedi, H., Mehrabi, M., Bui, D.T., Pradhan, B. and Foong, L.K. (2020), "Fuzzy-metaheuristic ensembles for spatial assessment of forest fire susceptibility", *J. Environ. Manag.*, **260**, 109867. https://doi.org/10.1016/j.jenvman.2019.109867

Moayedi, H., Ghareh, S. and Foong, L.K. (2021), "Quick integrative optimizers for minimizing the error of neural computing in pan evaporation modeling", *Eng. Comput.*, **38**, 1331-1347. https://doi.org/10.1007/s00366-020-01277-4

Moazenzadeh, R., Mohammadi, B., Shamshirband, S. and Chau, K.W. (2018), "Coupling a firefly algorithm with support vector regression to predict evaporation in northern Iran", *Eng, Applicat. Computat. Fluid Mech.*, **12**(1), 584-597. https://doi.org/10.1080/19942060.2018.1482476

Mohammadrezapour, O., Piri, J. and Kisi, O. (2019), "Comparison of SVM, ANFIS and GEP in modeling monthly potential evapotranspiration in an arid region (Case study: Sistan and Baluchestan Province, Iran)", *Water Supply*, **19**(2), 392-403. https://doi.org/10.2166/ws.2018.084

Moré, J.J. (1978), *Numerical Analysis*, Springer, pp. 105-116.

Muhammad, M.K.I., Nashwan, M.S., Shahid, S., Ismail, T.B., Song, Y.H. and Chung, E.S. (2019), "Evaluation of empirical reference evapotranspiration models using compromise programming: a case study of Peninsular Malaysia", *Sustainability*, **11**(16), 4267. https://doi.org/10.3390/su11164267

Nehdi, M. and Greenough, T. (2007), "Modeling shear capacity of

RC slender beams without stirrups using genetic algorithms", *Smart Struct. Syst., Int. J.*, **3**(1), 51-68. https://doi.org/10.12989/sss.2007.3.1.051

Nguyen, H., Mehrabi, M., Kalantar, B., Moayedi, H. and Abdullahi, M.A.M. (2019), "Potential of hybrid evolutionary approaches for assessment of geo-hazard landslide susceptibility mapping", *Geomat. Natural Hazards Risk*, **10**(1), 1667-1693. https://doi.org/10.1080/19475705.2019.1607782

Pinkus, A. (1999), "Approximation theory of the MLP model in neural networks", *Acta numerica*, **8**, 143-195. https://doi.org/10.1017/S0962492900002919

Qasem, S.N., Samadianfard, S., Kheshtgar, S., Jarhan, S., Kisi, O., Shamshirband, S. and Chau, K.W. (2019), "Modeling monthly pan evaporation using wavelet support vector regression and wavelet artificial neural networks in arid and humid climates", *Eng. Applicat. Computati. Fluid Mech.*, **13**(1), 177-187. https://doi.org/10.1080/19942060.2018.1564702

Rao, R.V., Savsani, V.J. and Vakharia, D.P. (2011), "Teaching–learning-based optimization: a novel method for constrained mechanical design optimization problems", *Comput.-Aided Des.*, **43**(3), 303-315. https://doi.org/10.1016/j.cad.2010.12.015

Riffi, M.E. and Bouzidi, M. (2015), "Discrete cuttlefish optimization algorithm to solve the travelling salesman problem", *Proceedings of 2015 3rd World Conference on Complex Systems* (*WCCS*), pp. 1-6. https://doi.org/10.1109/ICoCS.2015.7483231

Roushangar, K. and Shahnazi, S. (2019), "Bed load prediction in gravel-bed rivers using wavelet kernel extreme learning machine and meta-heuristic methods", *Int. J. Environ. Sci. Technol.*, **16**(12), 8197-8208. https://doi.org/10.1007/s13762-019-02287-6

Salih, S.Q., Allawi, M.F., Yousif, A.A., Armanuos, A.M., Saggi, M.K., Ali, M., Shahid, S., Al-Ansari, N., Yaseen, Z.M. and Chau, K.W. (2019), "Viability of the advanced adaptive neuro-fuzzy inference system model on reservoir evaporation process simulation: case study of Nasser Lake in Egypt", *Eng. Applicat. Computat. Fluid Mech.*, **13**(1), 878-891. https://doi.org/10.1080/19942060.2019.1647879

Sanikhani, H., Kisi, O., Nikpour, M.R. and Dinpashoh, Y. (2012), "Estimation of daily pan evaporation using two different adaptive neuro-fuzzy computing techniques", *Water Resour. Manag.*, **26**(15), 4347-4365. https://doi.org/10.1007/s11269-012-0148-4

Sayari, S., Mahdavi-Meymand, A. and Zounemat-Kermani, M. (2020), "Prediction of critical velocity in pipeline flow of slurries using TLBO algorithm: a comprehensive study", *J. Pipeline Syst. Eng. Practice*, **11**(2), 04019057. https://doi.org/10.1061/(ASCE)PS.1949-1204.0000439

Shimi, M., Najjarchi, M., Khalili, K., Hezavei, E. and Mirhoseyni, S.M. (2020), "Investigation of the accuracy of linear and nonlinear time series models in modeling and forecasting of pan evaporation in IRAN", *Arab. J. Geosci.*, **13**(2), 59. https://doi.org/10.1007/s12517-019-5031-7

Termeh, S.V.R., Kornejady, A., Pourghasemi, H.R. and Keesstra, S. (2018), "Flood susceptibility mapping using novel ensembles of adaptive neuro fuzzy inference system and metaheuristic algorithms", *Sci. Total Environ.*, **615**, 438-451. https://doi.org/10.1016/j.scitotenv.2017.09.262

Tikhamarine, Y., Malik, A., Kumar, A., Souag-Gamane, D. and Kisi, O. (2019), "Estimation of monthly reference evapotranspiration using novel hybrid machine learning approaches", *Hydrol. Sci. J.*, **64**(15), 1824-1842. https://doi.org/10.1080/02626667.2019.1678750

Xu, C.Y., Gong, L., Jiang, T., Chen, D. and Singh, V.P. (2006), "Analysis of spatial distribution and temporal trend of reference evapotranspiration and pan evaporation in Changjiang (Yangtze River) catchment", *J. Hydrol.*, **327**(1-2), 81-93. https://doi.org/10.1016/j.jhydrol.2005.11.029

Yaseen, Z.M., Ehteram, M., Sharafati, A., Shahid, S., Al-Ansari, N. and El-Shafie, A. (2018), "The integration of nature-inspired algorithms with least square support vector regression models: application to modeling river dissolved oxygen concentration", *Water*, **10**(9), 1124. https://doi.org/10.3390/w10091124

Yaseen, Z.M., Faris, H. and Al-Ansari, N. (2020), "Hybridized extreme learning machine model with salp swarm algorithm: a novel predictive model for hydrological application", *Complexity*, **2020**. https://doi.org/10.1155/2020/8206245

Ye, X., Moayedi, H., Khari, M. and Foong, L.K. (2020), "Metaheuristic-hybridized multilayer perceptron in slope stability analysis", *Smart Struct. Syst., Int. J.*, **26**(3), 263-275. https://doi.org/10.12989/sss.2020.26.3.263

Zeinolabedini Rezaabad, M., Ghazanfari, S. and Salajegheh, M. (2020), "ANFIS modeling with ICA, BBO, TLBO, and IWO optimization algorithms and sensitivity analysis for predicting daily reference evapotranspiration", *J. Hydrol. Eng.*, **25**(8), 04020038. https://doi.org/10.1061/(ASCE)HE.1943-5584.0001963

Zhang, Y., Jin, Z. and Chen, Y. (2020), "Hybrid teaching–learning-based optimization and neural network algorithm for engineering design optimization problems", *Knowledge-Based Syst.*, **187**, 104836. https://doi.org/10.1016/j.knosys.2019.07.007

Zhang, Y., Liu, L., Zhu, Y., Wang, P. and Foong, L.K. (2022), "Novel integrative soft computing for daily pan evaporation modeling", *Smart Struct. Syst., Int. J.*, **30**(4), 421-432. https://doi.org/10.12989/sss.2022.30.4.421

Zhou, G., Moayedi, H. and Foong, L.K. (2020), "Teaching–learning-based metaheuristic scheme for modifying neural computing in appraising energy performance of building", *Eng. Comput.*, **37**, 3037-3048. https://doi.org/10.1007/s00366-020-00981-5

CC